

A&A manuscript no.
(will be inserted by hand later)

Your thesaurus codes are:
02.01.2;02.02.1;11.10.1;11.17.3

ASTRONOMY
AND
ASTROPHYSICS
30.9.2018

The symbiotic system in quasars: black hole, accretion disk and jet

Alina-Cătălina Donea^{1,2} and Peter L. Biermann¹

¹ Max-Planck-Institut für Radioastronomie, Auf dem Hügel 69, D-53121 Bonn, Germany

² Astronomical Institute of the Romanian Academy, Cușitul de Argint 5, RO-75212, Bucharest, Romania

received date; accepted date

Abstract. The UV continuum spectrum of quasars and AGN is assumed to originate from an accreting disk surrounding a massive rotating black hole. We discuss the structure and emission spectra of a disk which drives a powerful jet. Due to the large efficiency of extracting energy from the accreting matter in the inner part of the disk close to the massive object, all the energetic conditions for the formation of jets are fulfilled. The total energy going up into the jet depends strongly on the Kerr black hole parameters, on the disk features and on the mass flow and thickness of the jet. The shape of UV spectra of the AGN can be explained by a sub-Eddington accretion disk which drives a jet in the innermost parts.

Key words: black holes, accretion disks, jets, UV-data of PG quasars

1. Introductory

The general concept of an AGN (active galactic nucleus) contains three important ingredients. The first constituent which binds the space-time geometry and dictates how the matter has to move in its vicinity is a black hole. The great luminosities observed depend on the masses of the black holes $M \in [10^8 M_\odot, 10^{10} M_\odot]$. The second one is the disk of gas. Matter flows towards the massive object following nearly circular orbits. The disk-like accretion onto a black hole is the most plausible explanation for the strong emission in the ultraviolet (UV), the so-called "big blue bump" (Shields 1978) and for the X-rays in AGN. The third component of an AGN is the jet. The notion that the jets and the accretion disks are symbiotically related originated since the first radio and optical observations revealed the parsec-scale of the AGNs. A geometrically thin disk with a mass accretion rate lower than the limit imposed by the Eddington accretion rate can drive outflows in the dense regions in the vicinity of a black hole. The flow can be ejected from the regions of the disk where the forces of the radiation

pressure, gas pressure and gravitation are comparable. Relativistic jets can extract high amounts of energy from the central object (Falcke and Biermann 1995). Pudritz (1986) proposed that an MHD jet could extract the angular momentum of the accretion disk, so that the jet can control the accretion process in the vicinity of the last marginally stable orbit. The jet-disk system is governed by the conservation laws of mass, angular momentum and energy.

2. The inner boundary conditions

We assume that the spacetime geometry where the disk develops is described by the Kerr metric. The mass of the black hole is M and its specific angular momentum is a . The geometry of the accretion disk is described by the radius R and its thickness H . The disk is geometrically thin ($H/R \ll 1$) and we work with the basic assumption that the accretion is quasisteady (Novikov and Thorne 1973, hereafter NT73) with a constant rate of mass accretion \dot{M} . The disk consists of fully ionized hydrogen and the effects of magnetic fields on the disk structure are neglected in our calculations. We consider the case that the disk is not self-gravitating and its rotation law is keplerian.

We assume that the jet starts between R_{ms} , the last, marginally stable orbit in the absence of a jet and the radius R_{jet} with $R_{jet} > R_{ms}$, extracting mass, energy and angular momentum from the disk. The presence of the jet will modify both the behaviour of infalling matter across the radius R_{jet} and the structure of the keplerian disk. The jets are placed in the potential well of a Kerr black hole. The rotating central object supplies, through its gravitational potential well, the energy necessary for driving and maintaining a stable jet in the AGNs. We consider the case that the gravitational potential energy released between the R_{ms} and the outer radius of the jet R_{jet} goes into the jet.

On the other hand, the geometry and the total energy of the jet are connected with the physical properties of the interior regions of the disk. Using the above mentioned premises we have to deal with a jet-disk symbiosis (Falcke and Biermann 1995): a "standard disk" (Shakura and Sunyaev 1973, hereafter SS73) and a powerful jet (Blandford and Königl 1979). Both

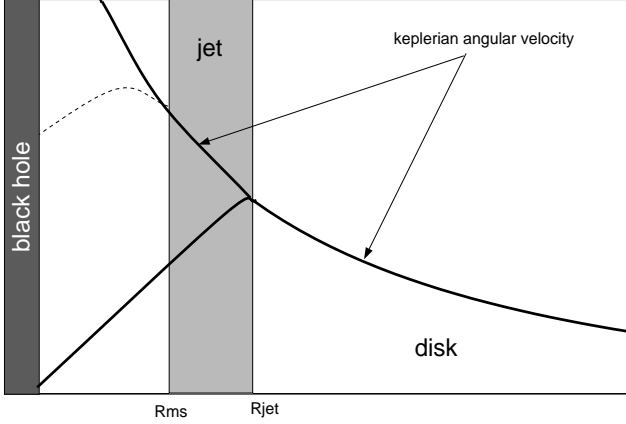


Fig. 1. Angular velocity via the radius of the disk. The shadowed zone indicates the innermost region of the disk where the jet is created. The thin-dashed line describes the behavior of the infalling matter if the disk can not drive the jet at its boundaries.

the disk and the jet structure are governed by the mass and the spin of the black hole.

The angular velocity of the accreting matter at the innermost boundaries will sharply decrease from $\Omega(R_{jet})$ to the angular velocity of the black hole, if we consider that a jet exists. The angular velocity of the black hole is unknown because the surface of infinite redshift (the horizon) hides the image of the massive black hole. Therefore, the massive rotating object has no solid surface on which the accreting matter can follow. The radius of the horizon is considered to be the surface of the black hole. We believe that $\Omega(R)$ will drop rapidly compared with the simple case of a disk and no jet (see Fig.1). The problem of the inner boundary conditions for the disk structure calculations is solved by using an approximate condition: $\frac{d\Omega(R)}{dR} = 0$ at $R = R_{jet}$. We assume that viscous stresses do not exist across the new boundary of disk.

In a first exploration of the physical consequences of the jet-disk symbiosis we use R_{jet} as our key parameter; it is obvious that a full treatment would have to model the detailed magnetohydrodynamics. However, whatever the details of any model, energy and mass conservation have to hold, and so we parametrize a range of possible models with R_{jet} , the radius where the transition from disk to jet occurs.

3. The connection between jet and disk

The unification scheme for all quasars and AGN suggests that one can not treat the disk and jet as two separate objects. The concept of a jet-disk symbiosis has been introduced by Falcke and Biermann (1995). In order to describe the reciprocal influences between the three principal objects : the black hole, the disk and the jet, we shall use a standard set of parameters (Falcke et al. 1995a), defining:

$$Q_{accr} = \dot{M}c^2, \quad (1)$$

$$q_m = \frac{\dot{M}_{jet}}{\dot{M}}, \quad (2)$$

$$q_j = \frac{Q_{jet}}{\dot{M}c^2}, \quad (3)$$

$$q_l = \frac{L_{disk}^{jet}}{\dot{M}c^2}. \quad (4)$$

Here \dot{M} is the rate of mass accretion rate in the disk. The mass flow rate into the jet is \dot{M}_{jet} . We assume that a jet exist on both sides of the disk, and use this symmetry in our quantitative modelling. Q_{jet} is the total power of the jet – including the rest energy of the expelled matter – and is expressed as:

$$Q_{jet} = L_{disk} - L_{disk}^{jet}, \quad (5)$$

L_{disk}^{jet} is the total luminosity of a disk modified by the presence of the jet and L_{disk} is the total luminosity of the disk if there are no physical conditions to drive the jet. A large fraction of the total power of the jet is in magnetic fields and relativistic particles.

The dimensionless parameters q_j , q_l and q_m have to be less than 1, because the jet can not consume more matter and energy than is provided by the accretion disk. pushed out into the jet will be swallowed by the black hole. The structure of the disk is strongly connected with a new characteristic length scale r_j defined as follows:

$$R_{jet} = R_{ms}(1 + r_j). \quad (6)$$

The parameter r_j is dimensionless and the null values for the q_m and r_j require the simple system with two components: the black hole and the disk.

4. Properties of the Kerr disk driving jet

For radii less than $30R_g$, where $R_g = GM/c^2$ is the gravitational radius we need to introduce the relativistic corrections (NT73) in order to describe the accretion disk around the Kerr black hole and the relativistic collimated jet.

We follow the methods of standard accretion disk theory (SS73), splitting the calculation of the disk structure into four parts: the analysis of mass, energy and angular momentum conservation for the disk-jet system, the structure of the disk and the propagation of radiation through the disk's z-layering. The z coordinate is parallel to the symmetry axis of the entire jet-disk system and perpendicular to the disk. The geometry of the disk is evaluated using the dimensionless parameters : $r_* \equiv R/R_g$ and $r_{jet*} \equiv R_{jet}/R_g$. The specific angular momentum of the black hole is represented by $a_* = a/R_g$.

We use the general relativistic correction factors denoted in Page and Thorne (1974), hereafter PT74, and NT73 as \mathcal{A} , \mathcal{B} , \mathcal{C} , \mathcal{D} , \mathcal{E} , \mathcal{F} , \mathcal{G} , \mathcal{J} in order to compute the quantities which describe the disk-jet symbiosis. These parameters have been used for simplicity of splitting formula into Newtonian part

plus the relativistic correction. They are functions of r_* and the parameter a_* . For $R \gg R_{ms}$ all factors mentioned tend to unity.

The radial structure of the disk is obtained by using the laws of conservation of rest mass, angular momentum and energy.

4.1. Rest-mass conservation

The rest-mass flowing inward through a cylinder of radius R in the time interval Δt , taking into account the flow along the jet is $\dot{M}\Delta t$, where \dot{M} is:

$$\dot{M} = -2\pi R \Sigma v^{\hat{R}} \mathcal{D}^{\frac{1}{2}} + \dot{M}_{jet}. \quad (7)$$

The radial function Σ is the surface density in the disk and $v^{\hat{R}}$ is the mass averaged infall velocity.

4.2. Angular-momentum conservation

The disk-like accretion is possible only if the angular momentum can be transported through the disk by some effective viscosity. The α viscosity law follows the prescriptions of SS73. The viscous torque is proportional to the pressure in the disk which depends on the jet and black hole parameters. We used a general constant value of 0.1 for the α parameter.

The additional loss of angular momentum into the jet modifies the conservation law of angular momentum in the disk as follows :

$$\left[-\dot{M}(1 - q_m) \tilde{L} + 2\pi R^2 \mathcal{B} \mathcal{C}^{-1/2} \mathcal{D} \mathcal{W} \right]_{,R} + 4\pi R \tilde{L} F + 2\pi R \dot{M}_{jet} \tilde{L}_{jet} = 0, \quad (8)$$

The integrated shear tensor \mathcal{W} is similar to that defined in NT73. F is the flux of emitted energy through the upper (lower) face of the disk and \tilde{L}_{jet} is the specific angular momentum extracted by the jet per unit surface.

The first term in the brackets is the angular momentum carried by the remaining mass of gas towards black hole determining the spin of the central object. The second term represents the angular momentum transported by the torques in the disk. The third and the fourth terms contain information about the angular momentum carried away by the radiation and, respectively, by the jet.

4.3. Conservation of energy

The gravitational potential energy is released in the disk through viscous dissipation of shear generated by differential rotation of the disk. The energy flux in the vertical direction is:

$$F = \frac{3}{4} \left(\frac{1}{M r_*^{3/2}} \right) \frac{\mathcal{D} \mathcal{W}}{\mathcal{C}} \quad (9)$$

Using the conservation laws for energy and angular momentum we get a differential equation for the integrated stress \mathcal{W}

with an additional term for the angular momentum extraction by the jet:

$$\left[-\dot{M}(1 - q_m) \tilde{L} + 2\pi R^2 \mathcal{B} \mathcal{C}^{-1/2} \mathcal{D} \mathcal{W} \right]_{,R} + 2\pi \frac{3}{2} \left(\frac{M}{R} \right)^{1/2} \tilde{L} \frac{\mathcal{D}}{\mathcal{C}} \mathcal{W} + 2\pi R \dot{M}_{jet} \tilde{L}_{jet} = 0, \quad (10)$$

The solution of the equation is straightforward. In order to solve more easily the differential equation (10) and to keep a similar form of the final result as that found by NT73, we define \mathcal{L}' and \mathcal{Q}' , two functions of r_* . Only, when we consider no-jet models we can get a form of these parameters equal to those of NT73. Due to the consideration of the jet in our model, the equation (10) includes the angular momentum extracted by the jet. The parameters: \mathcal{L}' and \mathcal{Q}' , depend on the presence of the jet, also. Hence,

$$\mathcal{L}' \equiv \frac{\tilde{L}(r_*) - \tilde{L}(r_{jet*})}{M r_*^{1/2}}, \quad (11)$$

$$\mathcal{Q}' \equiv (1 - q_m) \mathcal{L}' - \frac{3}{2 r_*^{1/2}} \mathcal{J} \tilde{I} \quad (12)$$

where \tilde{I} is:

$$\tilde{I} \equiv \int_{r_{jet*}}^{r_*} \left[(1 - q_m) \frac{\mathcal{F}}{\mathcal{B} \mathcal{C}} \frac{\mathcal{L}'}{\mathcal{J}} \frac{1}{r_*^{3/2}} + \frac{2}{3} \frac{q_m}{M} \frac{\tilde{L}_{jet}}{\mathcal{J}} \right] d\tilde{r}_* \quad (13)$$

$\tilde{L}(r_{jet})$ is the angular momentum per unit mass for the circular orbit at $R = R_{jet}$. The case of the disk without the jet is obtained if $r_j \rightarrow 0$, $q_m \rightarrow 0$ and if the inner boundary is fixed by the limit $r_{jet*} \rightarrow r_{ms*}$. The dimensionless parameter for the innermost stable orbit is $r_{ms*} \equiv R_{ms}/R_g$.

The constant of integration is found from the condition that no viscous stresses act across the boundary $R = R_{jet}$. The amount of the energy dissipated per unit area in unit time is computed using the new \mathcal{L}' and \mathcal{Q}' parameters defined above and has a similar form comparing to that found by NT73 :

$$F = \frac{3G}{8\pi} \frac{\dot{M}}{M^2} \frac{1}{r_*^3} \frac{\mathcal{Q}'}{\mathcal{B} \mathcal{C}^{1/2}}, \quad (14)$$

with the new \mathcal{Q}' and \mathcal{L}' parameters defined above.

In Fig. 2 we show the energy dissipation released into the disks surrounding rotational or stationary black holes. The thick lines correspond to disks placed in a Kerr geometry.

The total luminosity from the two sided-disk which gives birth to the jet is given by integration over the disk surface:

$$L_{disk}^{jet} = 4\pi \int_{R_{jet}}^{R_{out}} F(R) R dR \quad (15)$$

If we keep a constant mass M and a constant mass accretion rate \dot{M} then it is obvious that for models with the same rotation

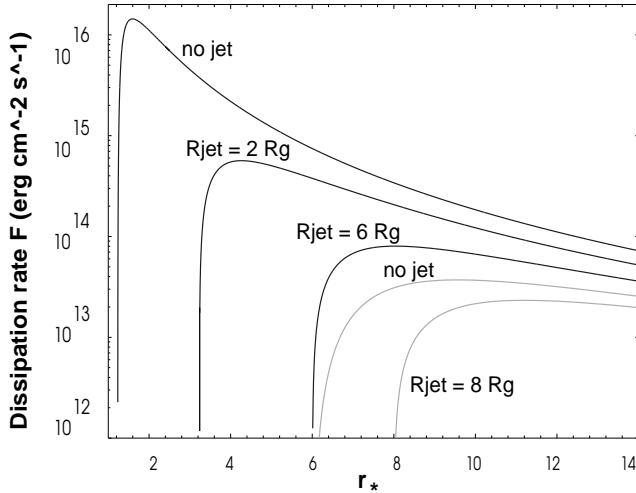


Fig. 2. The energy dissipation rate F against the dimensionless parameter r_* . The thick lines correspond to the case of a maximally rotating black hole and the thin lines correspond to the Schwarzschild black hole. The mass of black hole is $M = 10^8 M_\odot$ and R_{jet} is the outer radius of the jet defined in text.

parameter, the liberated fluxes are smaller for systems driving jets compared with those that do not (see Fig. 2). We plot the energy fluxes released by the Kerr disk with a jet for two different outer radii of the jet: $R_{jet} = 2R_g$ and $R_{jet} = 6R_g$. The bigger the base of the jet, the larger the amount of energy going into jet.

If one asks for a geometrical disk with the innermost Keplerian orbit at $6R_g$, we can choose the system consisting of: maximal Kerr black hole, a jet starting between $1.23R_g$ and $6R_g$ and the outer disk (see Fig. 2). One can see that this particular model replaces the simple case of a Schwarzschild black hole and a disk without jet. The comparison of these two models leads to the conclusion that the energy liberation rate in the disk with the jet surrounding a Kerr black hole is greater than the energy dissipation rate in a simple disk surrounding a stationary black hole, when both the disks have equal inner radii. The release of gravitational energy can be explained with these symbiotic systems. This is the key result which allows the fits to observed spectra shown below.

The precipitous drops in the radiative flux, when jets are present for different spins of black holes are straight results emerging from our assumptions that the gravitational potential energy released between the R_{ms} and the outer radius of the jet R_{jet} goes into the jet. This sharp drop is easily understood, if one considers the Kerr disk as reference: it arises from cutting a Kerr disk off at R_{jet} . The Keplerian disk does not exist anymore inside R_{jet} .

5. Spectrum of the disk

The disk has three distinct regions pointed out by SS73: the dominant radiation pressure inner zone, the dominant electron

scattering zone and the gas pressure and free-free absorption external zone.

The boundary radii describing the transitions between the three distinct regions of the relativistic disk with the jet surrounding a maximal Kerr black hole are smaller than those found for the disk which does not drive the jets in the same spacetime. It means the regions where the radiation pressure dominates are small, and extend to moderate radii close to the footpoint of the jet.

The radiation pressure can not dominate the gas pressure in the interior zones of the disks, if the mass accretion rates are small and the outflowing jets have thick bases and large mass fluxes.

The final analytical formulae for the complete structure of the relativistic disk are similar to those derived in NT73 but with our new \mathcal{L}' and \mathcal{Q}' parameters replaced, for all three regions with different physical properties. If the disk is optically thick and absorption dominates over scattering, the local emission from the disk can be described by a Planck blackbody function with an effective temperature:

$$T_{eff} = \left(\frac{F(r_*)}{\sigma} \right)^{1/4} \quad (16)$$

In Fig.3 we plot the density ρ_0 , the effective temperature T_{eff} and the z_0 half-thickness for different innermost zones of the relativistic disks. We take $\dot{M} = 0.01 M_\odot / yr$, the mass of the black hole $M = 10^8 M_\odot$ and the dimensionless parameter of the specific maximum angular momentum $a_* = (0, 0.9981)$. The structure of the disk with no jet and that of a disk with a jet starting between $6R_g$ and $10.77R_g$, surrounding a Schwarzschild black hole is shown in Fig 3. with thin lines.

As we expect, one observes in Figures 2 and 3, that the simple rotating models containing only a Kerr black hole and a disk (case a) are luminous and hotter than those with stationary black holes (case c). The case b) corresponds to the system: a Kerr black hole, disk and a jet between $1.23R_g$ and $6R_g$.

By comparison of the case a) with outflow and the case b) with no outflow, we see that the disk is denser and thinner in the second case. We use the same rotation parameter a_* . The thicker the base of the jet the thinner is the new disk. The effective temperatures could decrease by one order in magnitude. A temperature of $10^{4.5} K$ in the radiation pressure zone is high enough in order to explain the Big UV-Bump observed in the AGNs spectra.

A jet between $1.23R_g$ and $6R_g$ leads to values of the densities and thickness of the new structure in the disk, similar to those computed for a simple disk in Schwarzschild geometry. These similarities permit to replace the simple systems, with the new one consisting of a powerful jet, a disk like and the central object.

The case d) in Fig. 3 shows the properties of a disk surrounding a Schwarzschild black hole. The thick jet in this example has the inner radius at $6R_g$ and the outer radius at $10.5R_g$.

The energies of the emitted photons from the disk are dependent on the opacities, the temperatures and the densities in

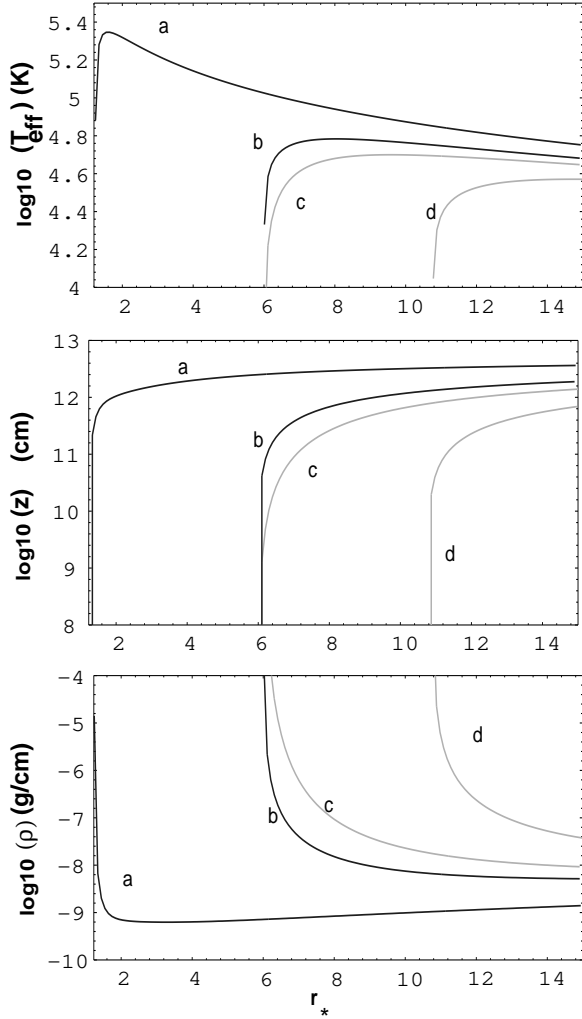


Fig. 3. The effective temperature T_{eff} , the density ρ_0 and the half-thickness z_0 of the inner part of the disk as functions of the dimensionless radius r_* for the similar cases mentioned in the Fig 2. The darker lines show the cases of the disks surrounding a Kerr black hole and the grey lines show the disks in Schwarzschild geometry. The cases a) and c) show the properties of the disk driving no jets. The cases b) and d) correspond to the jets with equal thicknesses of $4.77R_g$.

the disk. At high frequencies the opacity in the disk is dominated by Thomson scattering and for the inner regions of disk the comptonization will modify the spectrum if the y parameter is large enough. In the inner regions of the disk the Compton parameter:

$$y = \frac{4kT_e}{m_e c^2} \tau_T^2 \quad (17)$$

has to be greater than 1 and depends on the electron temperature and the Thompson optical depth $\tau_T = k_T \rho z_0$ where k_T is the Thompson opacity coefficient. The mass and energy loss into the jet lead to a shrinking region of electron scattering dominant opacity. A thick base of the jet can cover the whole region

in which comptonization can harden the blackbody photons emitted in a disk which has no jet.

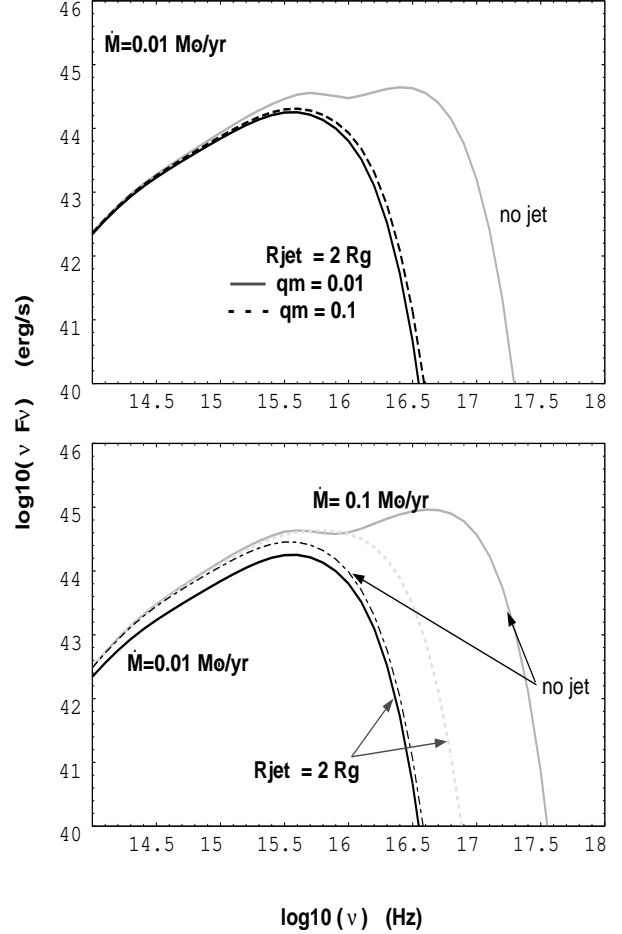


Fig. 4. Emergent spectra for $M = 10^8 M_\odot$ and $\dot{M} = 0.01 M_\odot / yr$. The light colored lines show the computed emergent spectra when the disk does not drive a jet, for different mass accretion rates. The continuous dark lines show the computed emergent spectrum when the disk drives a jet with $R_{jet} = 2R_g$, and $q_m = 0.01$. The thin dark dotted line in the second graph shows a spectra emerging from a disk that does not drive a jet, for a small $a_* = 0.7$.

It is not clear if the disk is thermally unstable in the inner regions of the relativistic disk. There are some questions which have to be solved: does the jet make these inner regions thermally unstable or does an initial thermally unstable disk become thermally stable due to the presence of the mass flowing into the jet? Are there the viscous instabilities in the relativistic disk with the jet?

The relativistic effects and the presence of jet modify the locally emitted spectrum. In Fig. 4 we plot the dependence of the emitted spectrum of the parameters q_m and r_j . In the optical

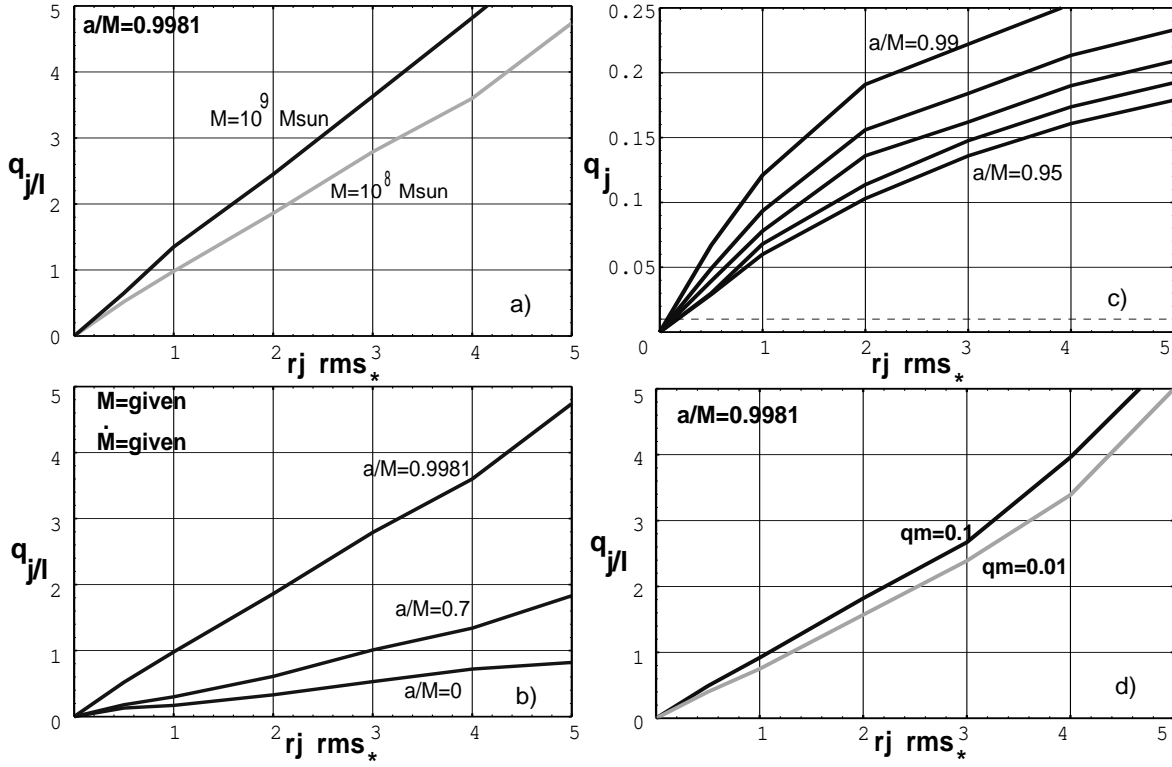


Fig. 5. Fig 5a: $q_{j/l}$ versus $r_j r_{ms*}$ for different masses M of black holes. Fig 5b: $q_{j/l}$ versus $r_j r_{ms*}$ for different spins of the black hole. Fig 5c: q_j versus $r_j r_{ms*}$ if the specific angular momentum of the black hole varies slowly between the values $[0.95, 0.99]$. Fig 5d: $q_{j/l}$ versus $r_j r_{ms*}$ for different mass flowing into the jet per unit time.

UV range the general form of the spectra is not significantly changed when the jets grow close to black holes. Most of the UV radiation originates from the inner region of disk outside the R_{jet} . Due to our theoretical assumption about the energy source of the jets, the form of the spectrum coming from an "old standard" disk rotating around a maximally rotating black hole is cut off at high frequencies, from EUV to soft X-ray range.

Our model contains two free parameters: q_m and r_j . The other two parameters q_j and q_l (relations (3) and (4)) concerning the energetics of our systems, are functions of q_m and r_j as we will see in the next section.

The range of variation of the first free parameter has to be between 0 and 1 (see Section 3). From the relativistic parametrized Bernoulli equation for the jet (Falcke et al. 1995b) one may deduce, if the jet velocity of the jet is known, the mass ratio q_m pushed out into the jet. We believe that a highest possible parameter q_m can be close to 0.1. Therefore, the emitted spectrum depends weakly on the parameter q_m (see Fig. 4).

The flattening of the spectra in the UV range due to the interactions between the blackbody photons and electrons in

the disk is slightly accentuated if we choose a thick base for the jet and a maximal ratio $q_m = 0.1$.

The second free parameter r_j provides information about the geometry of the footpoint of the jet. The range of variation of r_j is limited by the straight condition of the case no-jet, where $r_j = 0$. From the observations we know what values should be expected for the UV luminosities for a certain quasar. A thicker base of the jet diminishes the integrated flux emerging from the disk. So, one can not choose any maximum possible values for the outer radius of the jet because the constraints introduced by the data points.

One can see from the graphs that emergent spectrum from the simple model of a disk surrounding a rotational black hole with $a_* = 0.7$ and a mass $M = 10^8 M_{\odot}$ is similar with the spectrum coming out from a Kerr disk with the jet.

We have many possibilities to explain the same UV data of the quasars with the general model consisting of: black hole, a disk and a jet. A higher accretion mass rate in the disk ($\dot{M} = 0.1 M_{\odot}/yr$) and a jet growing (see Fig.4b) between $1.23 R_g$ and approximately $3 R_g$ determine a final form of the emitted spectrum identical with that computed for the

$\dot{M} = 0.01 M_{\odot}/\text{yr}$ and $R_{jet} = 2R_g$. We can also reach a similar form if we take the simplest model of a black hole with a smaller spin ($a_{*} = 0.7$) and a thin disk (see Fig.4). We can therefore obtain good fits at different mass accretion rate and different radii of the jet in the maximal Kerr geometry.

6. The energetics of the jet

We consider that the flow of matter absorbed by a supermassive black hole is the primary source for mass outflows in the inner dense part of a disk. Many different types of mechanisms have been proposed for the formation of the jets. We note here the jet model driven by thermal or radiation pressure (Lovelace et al. 1994) or the formation of the jet due to the magnetic activity of the accretion disks (Camenzind 1986). We do not wish to propose an explanation of the jet formation. We show that some information about the size of the formation region and the energy of the jet can be inferred studying the emitted flux from the accreting disk.

We have defined in the third section q_j as the ratio between the total power gained by the jet and the rest energy at infinity of the matter $\dot{M}c^2$. The Fig. 5 shows how the total energy of the jet is connected with its geometrical parameter r_j . The greater the specific angular momentum and the mass of black hole, the more powerful is the jet (see Figs. 5a and 5b).

The dimensionless parameter $q_{j/l}$ defined below, gives the ratio between the total jet power and the disk luminosity:

$$q_{j/l} = \frac{Q_{jet}}{L_{disk}^{jet}} \quad (18)$$

The total power gained by the jet Q_{jet} varies with the size of the starting area, respectively with r_j and depends slowly on the dimensionless parameter q_m which gives information about the mass loss rate into the jet (see Fig. 5d). The disk luminosity L_{disk}^{jet} is equal to the total energy pushed into the jet Q_{jet} if the jet has a thickness given by the product $r_j \cdot r_{ms*} = 1$, where $r_{ms*} = 1.23$ for a maximal Kerr black hole. A large accretion rate of the disk makes the jet strong. At the boundary zone, the structure of the old disk is destroyed. A fast rotating starved black hole attracts the gas matter so strongly that a big fraction $(1 - q_m)\dot{M}$ can not be saved by the jet from the inevitable swallowing.

We imagine that at the formation of the escaping jet the flow occurs through a cylinder with $R_{min} = R_{ms}$ and $R_{out} = R_{jet}$ (we shall call that "base of the jet") and then begins to expand covering the inner part of the disk.

The kinetic energy in the jet has to be great enough in order to provide all sources of energy required by the nonthermal processes. The total power going into the jet is limited by the Eddington disk luminosity. The energetic processes which we assume to occur in the jet are: particle acceleration by shocks, hadronic interaction between energetic protons and photons from the disk (Mannheim 1995) as well as between energetic protons and the accretion disk (Niemeyer and Biermann, 1996). In this latter model the energetic protons are created at the boundary of a nuclear jet and then diffuse towards the disk to

finally produce the hard X-ray spectra of the Seyfert galaxies. The hadronic reactions require a powerful jet which should be able to transport energy far away from the disk equatorial zone.

We do not include in our computation the influence on the disk spectrum coming from a possible hot corona (Haardt and Maraschi 1991) which should be situated on the top of the disk layer. We do not know the height of the base of jet which can be totally immersed in an optically thin, hot corona and therefore can influence the comptonized UV disk photons.

7. Theory and observations

A study of a large sample of quasars suggests that our model agrees with data. We present here the sample of the six PG quasars examined in the soft and hard X-ray domains by Rachen et al. (1995, hereafter RMB95).

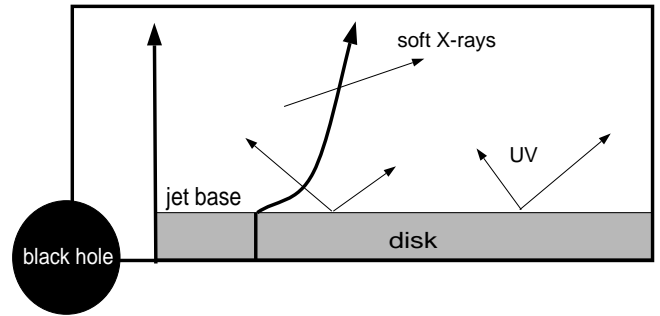


Fig. 6. The simple geometry of the symbiotic system: black hole, accretion disk and the jet.

We adopt Mannheim's model (Mannheim et al. 1995) to explain the existence of the soft X-ray emission (see Fig. 6). If the base of jet is surrounded by the UV radiation field it is expected that these photons will heat the base of jet, and after repeated Compton-scatterings with the hot thermal electrons in jet, they will become hardened. The unsaturated comptonization will produce a power-law extension of the UV bump spectrum. The resulting spectral index depends sensitively on the Compton y parameter which must be close to 0.5. The thickness of the jet limits the maximum energy of the UV photons which will hit the base of the jet.

The X-ray data of the all six quasars can be fitted very well by double power law spectra. RMB95 pointed out that there is a soft X-ray power law spectrum with an averaged observed spectral slope: $\alpha_{sx} = 2.1 \pm 0.3$. A flatter hard X-ray power law ($\alpha_{hk} \simeq 1$ for radio-weak AGN and $\alpha_{hk} \simeq 0.7$ for radio-louds) cross with the soft X-ray power law at a break energy close to the value $1.4 \pm 1.1 \text{ KeV}$. Friedrich (1994) gives detailed information about the X-ray data of the quasars, including a statistical description of the soft and hard power law slopes.

Our model fits well all the data in the UV range if we choose large masses for rotating black holes, sub-Eddington accretion

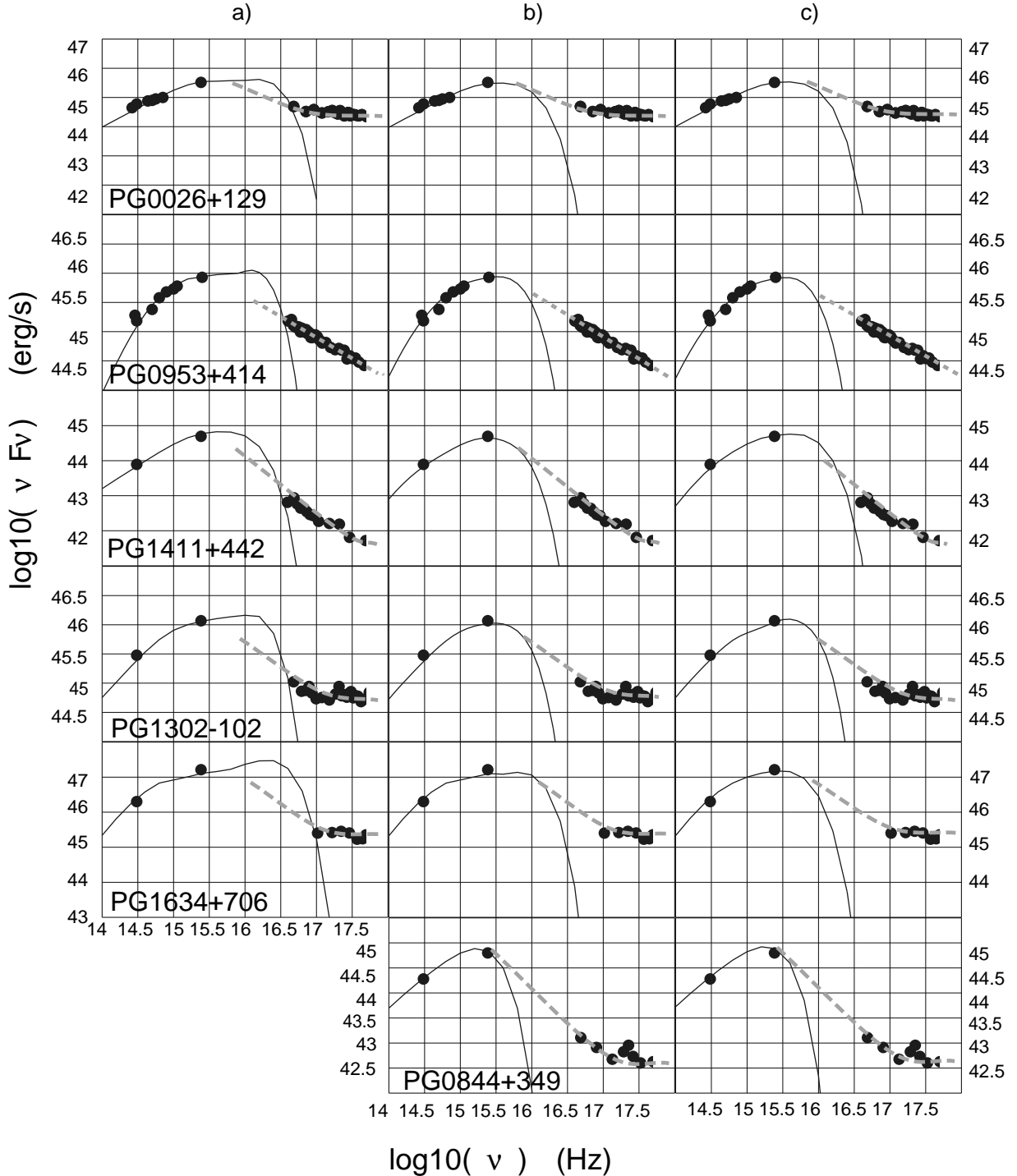


Fig. 7. Spectral energy distribution of the PG quasars in their source frame. The solid lines show the theoretical spectra of the relativistic accretion disk driving the jet in the interior regions. The dashed curves try to fit the X-ray data taking into account the the break energy where the soft and hard X-ray power law intersect (see text). The a) case plots the luminosity of an accretion disk with the jet surrounding a maximal Kerr black hole so as to have an intersection point between the fit-curve of the spectrum of the disk and the soft X-ray data. In the b) case we have a powerful extreme jet. The intersection points between the solid lines and the dashed curves are "pivot point" for all lines which try to fit the soft X-ray data. The c) case represents the luminosities of the disk around a slowly rotating black hole for the simple case of a disk which does not drive a jet. The UV continuum data are from Mannheim et al. (1995), Malkan (1989) and Laor (1990). The soft X-ray data points are from the RMB95. The Hubble constant adopted has the value $H_0 = 50$ km/s/Mpc.

rates and powerful jets with $r_j \cdot r_{ms*} \in [0.2, 5.5]$. The first case a) in Fig 7. corresponds to the "Kerr maximum" case because we have chosen the dimension of the escaping jet so that we wish to have an intersection point between the fit-curve of the spectrum of the disk and the soft X-ray data. We assume that the disk photons with energies above the energy corresponding to the intersection point will be comptonized in the jet producing the slope observed in the soft X-ray domain of the majority of quasars.

of these six quasars. X-ray data of the soft and hard power law hard X-ray power law slope and $\alpha_{hk} \simeq 0.7$ for data situated below the break energies which soft and hard X-ray power law intersect (RMB95), in connection between our model and the Mannheim's model. Above energies a horizontal line will fit the hard X-ray data points.

Using the unsaturated comptonization at the base of jet we could find other possible solutions in order to explain the continuity from the "big blue bump" to the hard X-ray domain.

The second case b) from the Fig. 7 belongs to the "maximal jet" possibility. In this figure we plot with dashes the possible curves which fit the X-ray data using the general averaged slopes emphasized by RMB95 and the respective break energy values of each quasar. The tangential line corresponding to the fit of soft X-ray data intersects the theoretical curve of the spectrum of the disk in a "pivot" point. This point can be the maximum of the luminosity of the disk. According to Mannheim's model the physical conditions at the base of the jet can influence the Compton parameter, implicitly the slope of the fit line in the soft X-ray range. We have a good fit of the UV data for all 6 quasars, in concordance with the disk model and a thicker base of the jet with $r_j \cdot r_{ms*} \in [1, 10]$. The spectra emerging from the disk are cut off at high energies having a maximum in the UV range. The value of the frequency corresponding with this maximum ν_{max} is correlated with the q_m and r_j parameters. A thick base of the jet diminishes the value of the frequency ν_{max} . The bigger the energy pushed into the jet, the smaller is the maximum photon energy coming from the disk. We can find the powerful possible case for the jets near a Kerr black hole with the specific angular momentum a_* .

The disk spectrum becomes softer when the black hole is rotating at $a_* < 0.9981$. That means, the jets will be poorly fed. The last c) case represents the luminosities of the disk around a slowly rotating black hole for the simple case of a disk which does not drive a jet in the innermost parts. We plotted the most extreme possible cases which can explain the UV data for quasars. This case requires the choice of the other models in order to explain the presence of the X-ray in quasars.

In Table 1 we present all parameters of the jets deduced for the 6 PG quasars. The dimensionless accretion rate \dot{m} is defined $\dot{m} \equiv \dot{M}/\dot{M}_{edd}$, where \dot{M}_{edd} is the Eddington mass accretion rate.

The radio-weak quasar PG0844+349 with a low redshift ($z < 0.1$) has the disk luminosity of $1.4 \cdot 10^{45}$ erg/s. We found that the jet extracts 40% of the total energy of the accreting matter. For a maximal Kerr black hole we get an extreme powerful jet with a thick base ($R_{jet} = 5R_{ms}$) and with its total energy

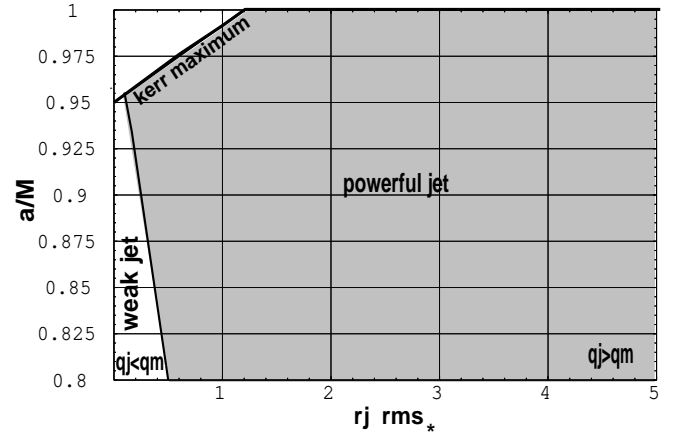


Fig. 8. The permitted area for a powerful jet starting close to a fast rotating black hole. Using our model we find that the minimum specific angular momentum possible for the black hole in the PG0953+414 quasar is dictated by the UV data. An angular momentum per unit mass a_* less than 0.8 is not allowed if we fit the UV data points.

$Q_{jet} = 9 \cdot 10^{45}$ erg/s. If we assume that the disk can not drive a jet in its dense regions and the black hole has a specific angular momentum which correspond to the value $a_* = 0.4$ and a mass of $6 \cdot 10^8 M_\odot$ the UV spectrum of this quasar can be explained too.

We work with sub-Eddington accretion rates in order to be in concordance with the starting assumption of a geometrically thin keplerian disk. A simple black body emission disk model which is rotating around a Schwarzschild black hole is not sufficient to explain the large UV fluxes for the quasars. In such a picture a large number of quasars require super-Eddington accretion rates.

In Fig. 8 we plot the permitted area for a strong jet in the PG 0953+414 quasar. The thick oblique line corresponds to the "kerr maximum" case for different specific angular momentum of black holes and different thickness of the base of jet. The shadowed zone covers the solution parameters which determine a good fitting of the UV data of the PG quasars if we take into account the comptonization of the radiation on the hot thermal electrons at the base of the jet.

We believe that only for fast rotating black holes with $a_* > 0.9$ and $r_j \cdot r_{ms*} > 1$ we may obtain the proper conditions at the base of jet to get unsaturated comptonized photons. For slowly rotating black hole and a geometrical thin base of the jet one gets small temperatures of electrons and small Thompson optical depths which can not explain the soft X-ray slope inferred from data points. The Compton parameter γ would be less than a general average value of 0.5 deduced by Mannheim et al. (1995). The condition $q_j > q_m$ comes from the energy and mass conservation laws along the jet. These physical conditions necessary to describe the jet base medium will be discussed in detail in a future paper.

Table 1. The fitting parameters of the 6 PG quasars for the three cases : a) Kerr maximum, b) Maximal jet, c) No jet and slowly rotating black holes

Source name	$\log_{10}Q_{jet}$	$\log_{10}L_{disk}^{jet}$	q_j	q_j/l	\dot{m}	a_*	$r_j \cdot r_{*ms}$	cases
PG0953+414	46.59	46.54	0.23	1.09	0.25	0.9981	1.2	kerr maximum
	46.73	46.30	0.32	2.67	0.25	0.9981	3	maximum jet
					0.25	0.8	0	no jet
PG0026+129	45.50	46.10	0.09	0.25	0.08	0.9981	0.2	kerr maximum
	45.92	45.87	0.24	1.10	0.08	0.9981	1	maximum jet
					0.08	0.95	0	no jet
PG1411+442	45.90	45.21	0.35	4.80	0.58	0.9981	5.5	kerr maximum
	45.95	44.89	0.39	11.4	0.58	0.9981	10	maximum jet
					0.58	0	0	no jet
PG1302-102	46.88	46.62	0.27	1.81	0.42	0.9981	2	kerr maximum
	46.96	46.23	0.33	3.42	0.42	0.9981	4	maximum jet
					0.42	0.8	0	no jet
PG1634+706	47.80	47.90	0.19	0.79	0.57	0.9981	0.8	kerr maximum
	48.02	47.60	0.31	2.64	0.57	0.9981	3	maximum jet
					0.57	0.6	0	no jet
PG0844+349	45.95	45.17	0.39	6.06	0.42	0.9981	5	maximum jet
						0.4	0	no jet

8. Summary

We have studied a symbiotic jet-disk system stationary in time. The jet is fed by a geometrically thin disk and we assumed that the inner part of the "standard" disk contains all energetic conditions necessary to form and to maintain a stable jet's configuration. The jet energy has the upper bound corresponding to the gravitational potential energy lost by the infalling gas between R_{ms} and R_{jet} .

The structure of the accreting disk is modified by the presence of the jet. The mass and angular momentum extraction from the disk makes it thinner and denser. The disk becomes cooler, especially in the regions close to the jet. Between the radius of the marginally stable circular orbit and the radius where it is assumed that a jet has the exterior edge R_{jet} we do not have a disk-structure any longer. A mass rate $q_m \dot{M}$ is pushed out into a powerful jet. We neglect the influence of the magnetic field in the structure of the disks and the jets. A very important step remains to be made. We would like to study in more details the vertical structure of a relativistic disk with a jet starting at its inner edge. A detailed analysis of a vertical structure of a relativistic disk surrounding a Schwarzschild black hole has been done by Dörrer (1995).

We demonstrate that our disk model driving a jet in the innermost dense regions very close to a maximal Kerr black hole can replace all the simple models of the accretion thin disk surrounding a Schwarzschild black hole.

The thickness of the jet given by the dimensionless parameter r_j is limited by the necessity to have sufficient UV photon flux in order to explain the high luminosity of the disk and the unsaturated comptonized photons in the base of jet.

The presence of the jet cuts off the high energy part of the spectrum of the disk without any jet (in the soft X-ray range) and its hot base comptonizes the photons coming from the disk.

The total energy carried out by the jet is strongly dependent on the mass and angular momentum of black hole.

We have shown that there is a strong correlation between the disk and the jet guided by the conservation laws of the mass, angular momentum and energy. The jet-disk connection leads to interesting models which explain the spectra of the quasars over the whole range of frequency. The assumption that the disk accretion is the machine which provides the energy in AGNs is the basic ingredient for all models mentioned.

Acknowledgements. A.D. would like to acknowledge receipt of a Max Planck fellowship which makes her work possible. We wish to thank Drs. H. Falcke, K. Mannheim and Jörg Rachen for intense and helpful discussions. P.B. would like to thank Drs. M. Romanova and R. Staubert for long and intense discussions of these points.

References

- Blandford R.D., Königl A. 1979, ApJ 232, 34
- Camenzind M. 1986, A&A 156, 137
- Dörrer T., 1995, PhD Thesis, Tübingen University
- Biermann P.L., 1993, A&A, A&A 241, 153
- Falcke H., Biermann P.L., 1995, A&A 293, 665
- Falcke H., Malkan M., Biermann P.L., 1995a, A&A 298, 395
- Falcke H., Gopal-Krishna, Biermann P.L., 1995b, A&A 298, 375
- Friedrich P., 1994, PhD Thesis, Tübingen University
- Haardt F., Maraschi L., 1991, ApJ 380, L51
- Ge J., 1995, to appear in ApJ.
- Laor A., 1990, Proceedings of the Sixth IAP Astrophysics Meeting / IAU Colloquium 129, "Structure and emission properties of accretion disks", ed. by C.Bertout et al. ApJ 335,57
- Lovelace V.E., Romanova M.M., Newman W.I., 1994, ApJ 437, 136
- Mannheim K., 1995, A&A 297, 321
- Mannheim K., Schulte M., Rachen J., 1995, A&A Letters 303, L41
- Niemeyer M., Biermann P.L., 1996, A&A, submitted

- Novikov I.D., Thorne K.S., 1973, Black Hole Astrophysics. In: DeWitt C., DeWitt B. (eds.), Les astres occlus, Gordon & Breach, New York, p.343-450, **NT73**
- Page D.N., Thorne K.S., 1974, ApJ 191, 499, **PT74**
- Pudritz R.E., 1986, ApJ 301, 571
- Rachen J., Mannheim K., Biermann P., 1995, A&A, in press, **RMB95**
Nat 349,
- Shakura N.I., Sunyaev R.A., 1973, A&A 24, 337, **SS73**
Eardley D.M., 1976,
- Shields, G.A., 1978, Nature 272, 706
- Sun W.H., Malkan M.A., 1989, ApJ 346, 68
A&A 143,374 Inoue H., Otani C., Dotani T., Hayashida K., Iwasawa K., Kii T., Kunieda K., Makino F., Matsuoka M., 1995, Nature 375, 659